

Magnetic-field-controlled spin valve and spin memory based on single-molecule magnets

Zhengzhong Zhang(张正中), Ruya Guo(郭儒雅), Rui Bo(薄锐), and Hao Liu(刘昊)
Citation: Chin. Phys. B, 2023, 32 (**9**): 097502. DOI: 10.1088/1674-1056/accf7c
Journal homepage: http://cpb.iphy.ac.cn; http://iopscience.iop.org/cpb

What follows is a list of articles you may be interested in

Unusual magnetic relaxation in a single-molecule magnet with toroidal magnetic moments

Dan Su(苏丹), Yi-Quan Zhang(张义权), En-Ke Liu(刘恩克), and Yang Sun(孙阳)
Chin. Phys. B, 2023, 32 (**8**): 087505. DOI: 10.1088/1674-1056/acd622

Bending sensor based on flexible spin valve

L I Naumova, R S Zavornitsyn, M A Milyaev, N G Bebenin, A Y Pavlova, M V Makarova, I K Maksimova, V V Proglyado, A A Zakharov, and V V Ustinov
Chin. Phys. B, 2023, 32 (**5**): 057502. DOI: 10.1088/1674-1056/ac8923

Probing the magnetization switching with in-plane magnetic anisotropy through field-modified magnetoresistance measurement

Runrun Hao(郝润润), Kun Zhang(张昆), Yinggang Li(李迎港), Qiang Cao(曹强), Xueying Zhang(张学莹), Dapeng Zhu(朱大鹏), and Weisheng Zhao(赵巍胜)
Chin. Phys. B, 2022, 31 (**1**): 017502. DOI: 10.1088/1674-1056/ac21bb

Bias-controlled spin memory and spin injector scheme in the tunneling junction with a single-molecule magnet

Zheng-Zhong Zhang(张正中) and Hao Liu(刘昊)
Chin. Phys. B, 2021, 30 (**6**): 067501. DOI: 10.1088/1674-1056/abd9b1

A new manganese-based single-molecule magnet with a record-high antiferromagnetic phase transition temperature

Cui Yan (崔岩), Li Yan-Rong (李艳荣), Li Rui-Yuan (李瑞元), Wang Yun-Ping (王云平)
Chin. Phys. B, 2014, 23 (**6**): 067504. DOI: 10.1088/1674-1056/23/6/067504

Magnetic-field-controlled spin valve and spin memory based on single-molecule magnets

Zhengzhong Zhang(张正中)[1,2,†], Ruya Guo(郭儒雅)[1], Rui Bo(薄锐)[1], and Hao Liu(刘昊)[1,‡]

[1] *Faculty of Mathematics and Physics, Huaiyin Institute of Technology, Huai'an* 223003, *China*
[2] *Nano Science and Technology Institute, University of Science and Technology of China, Suzhou* 215123, *China*

(Received 17 January 2023; revised manuscript received 10 April 2023; accepted manuscript online 24 April 2023)

A single-molecule magnet is a long-sought-after nanoscale component because it can enable us to miniaturize nonvolatile memory storage devices. The signature of a single-molecule magnet is switching between two bistable magnetic ground states under an external magnetic field. Based on this feature, we theoretically investigate a magnetic-field-controlled reversible resistance change active at low temperatures in a molecular magnetic tunnel junction, which consists of a single-molecule magnet sandwiched between a ferromagnetic electrode and a normal metal electrode. Our numerical results demonstrate that the molecular magnetism orientation can be manipulated by magnetic fields to be parallel/antiparallel to the ferromagnetic electrode magnetization. Moreover, different magnetic configurations can be "read out" based on different resistance states or different spin polarization parameters in the current spectrum, even in the absence of a magnetic field. Such an external magnetic field-controlled resistance state switching effect is similar to that in traditional spin valve devices. The difference between the two systems is that one of the ferromagnetic layers in the original device has been replaced by a magnetic molecule. This proposed scheme provides the possibility of better control of the spin freedom of electrons in molecular electrical devices, with potential applications in future high-density nonvolatile memory devices.

Keywords: single-molecule magnet, spin dependent electron tunneling, spin valve

PACS: 75.50.Xx, 75.60.Jk, 85.75.–d **DOI:** 10.1088/1674-1056/accf7c

1. Introduction

Spintronics aims to exploit the spin degree of freedom in solid-state devices for data storage and information processing technologies.[1] The spin valve (SV), a principal spintronic device, is a microelectronic device in which high-resistance (HR) and low-resistance (LR) states are realized by using both the charge and spin of carriers.[2,3] A standard magnetoresistance (MR) SV is an electronic device in which two conducting magnetic layers are separated by a nonmagnetic layer.[4,5] By applying an external magnetic field, considerable resistance switching can be achieved in the device by altering the magnetic configuration of the electrodes between parallel/LR and antiparallel/HR states. To date, various SV devices have been successfully manufactured, and the discoveries of giant magnetoresistance[6] (GMR) and tunneling magnetoresistance[7] (TMR) in metallic SV devices have revolutionized applications such as magnetic recording and memory.

Generally, the magnetic layers in SV devices are composed of ferromagnetic (FM) metals. With the development of materials science, molecule/organic-based magnets, which allow chemical tuning of electronic and magnetic properties, have become a promising new class of magnetic materials for future spintronic applications.[8–13] Among these magnets, single-molecule magnets[14–17] (SMMs), a new type of quantum magnetic material, have attracted increasing attention for their potential applications in novel spintronic devices.[18–20] The inner magnetic core of these molecules is surrounded by organic ligands, and the interaction between the magnetic cores of neighboring molecules is very weak, which leads to a large ground-state spin of SMMs.[21,22] This large ground-state spin of an SMM results in a double-well energy potential, which can resist magnetization reversal under low-temperature conditions.[17,23,24] Experimentally, electron transport of SMMs was observed with scanning tunneling microscopy and mechanically controllable break junctions,[25–30] although some results remain to be clarified.[31–35] More importantly, some studies have shown that electronic properties of these special molecules can be precisely controlled by electrical or magnetic means.[36–40] To date, many interesting phenomena of electron transport through SMMs have been discussed, such as spin blockade effect,[41,42] spin diode effect,[43,44] spin-Seebeck effect,[45,46] spin torque effect,[47–49] Kondo effect,[50–52] and superconducting effect.[53] According to studies of Bogani *et al.*, these molecules will be trapped in one of two metastable ground states $\pm S$, and only electrons whose spin direction is parallel to the molecular magnetism can pass through the SMM, resulting in high spin polarization of the tunneling current.[54] Due to this property, SMMs seem to be appropriate candidates for designing nanoscale spintronic devices, for example, spin

†Corresponding author. E-mail: zeikeezhang@163.com
‡Corresponding author. E-mail: hyitliuh@163.com

© 2023 Chinese Physical Society and IOP Publishing Ltd

filters or SV devices.[55,56]

In this work, we observe a spin-valve-like signal in our SMM-magnetic tunnel junction (MTJ) system, which consists of a magnetic molecule sandwiched between an FM lead and a nonmagnetic (NM) lead. A small detecting bias voltage is applied between two electrodes, and the conducting electrons are controlled by adjusting the external magnetic field. We observe a stable LR state under positive applied magnetic fields, a stable HR state under negative fields and HR–LR switching depending on the magnetization reversal of the SMM. Although much work on the spin-resolved transport properties of SMM molecules has been performed,[57–61] studies about the HR–LR switching effect controlled by magnetic signals in an SMM and the corresponding properties remain lacking. This work aims to fill this gap.

2. Model and Hamiltonian

As shown in Fig. 1(a), the magnetic molecular junction we consider here consists of an SMM placed between two metallic electrodes in the presence of an external magnetic field. The total Hamiltonian of this structure is composed of two parts, i.e., $H_{\rm total} = H_{\rm orbit} + H_{\rm spin}$,[41,62]

$$H_{\rm orbit} = \sum_{\sigma} \varepsilon_0 \hat{n}_\sigma + U\hat{n}_\uparrow \hat{n}_\downarrow + \sum_{\boldsymbol{k},\sigma,\alpha} (t_\alpha a^\dagger_{\alpha\boldsymbol{k}\sigma} c_\sigma + {\rm H.c.}) + \sum_{\boldsymbol{k},\sigma,\alpha} \varepsilon_{\boldsymbol{k}\sigma} a^\dagger_{\alpha\boldsymbol{k}\sigma} a_{\alpha\boldsymbol{k}\sigma}, \tag{1}$$

$$H_{\rm spin} = -DS_z^2 - \frac{J}{2}(S_+ s_- + S_- s_+ + 2S_z s_z) + H_{\rm M}. \tag{2}$$

Here, the first part $H_{\rm orbit}$ is the Hamiltonian of a typical single-molecule transistor; ε_0 is the energy of lowest unoccupied molecular orbital (LUMO), U represents the Coulomb interaction between the two electrons occupying the level; $\hat{n}_\sigma = c^\dagger_\sigma c_\sigma$ is the number operator, $\sigma = \uparrow (\downarrow)$ is the spin index, $a^\dagger_{\alpha\boldsymbol{k}\sigma}$ ($a_{\alpha\boldsymbol{k}\sigma}$) is the creation (annihilation) operator for the electron of momentum $\boldsymbol{k}$, spin σ in lead α; $c^\dagger_\sigma$ (c_σ) denotes the electron creation (annihilation) operator on the LUMO level; t_α describes the tunneling amplitudes for charging and discharging events between lead α and the molecule, which are assumed to be independent of momentum $\boldsymbol{k}$ and spin σ.

The second part $H_{\rm spin}$ is the spin Hamiltonian of the SMM with a giant local spin S and a magnetic uniaxial anisotropy constant D. J is the exchange coupling between the SMM and an electron in the LUMO. Here, $\boldsymbol{s} = \sum_{\sigma\sigma'} c^\dagger_\sigma \xi_{\sigma\sigma'} c_{\sigma'}/2$, with $\xi_{\sigma\sigma'}$ being the matrix element of the Pauli spin matrices. $S_\pm = S_x \pm {\rm i}S_y$ (similarly to $s_\pm$) are spin-raising operators, and $S_z(s_z)$ is the z component of the spin operator, with the z direction chosen along the magnetic easy axis. According to Refs. [41,46,48], the magnetic anisotropy perpendicular to the easy axis is usually smaller than D by several orders in magnitude and so is disregarded generally in $H_{\rm spin}$. $H_{\rm M} = -\Delta H(s_z + S_z)$ describes the Zeeman splitting energy induced by the external magnetic field along magnetic easy axis, where the $\boldsymbol{g}$ factor and the Bohr magneton $\mu_{\rm B}$ have been absorbed into ΔH.

Following the work reported in Refs. [48,63–65], the eigenstates of this structure can be denoted as $|n,m\rangle$, where $n = 0$, 1, or 2 is the number of electrons at the lowest unoccupied molecular orbital (LUMO) level, and m is the magnetic quantum number of $\boldsymbol{S}_{\rm T} = \boldsymbol{S} + \boldsymbol{s}$. The eigenenergies are given by $\varepsilon_{|0,m\rangle} = -\mathcal{D}m^2 - \Delta Hm$ for eigenstate $|0,m\rangle$, $\varepsilon_{|2,m\rangle} = 2\varepsilon_0 + U - \mathcal{D}m^2 - \Delta Hm$ for eigenstate $|2,m\rangle$, and $\varepsilon_{|1,m\rangle^\pm} = \varepsilon_0 + J/4 - \mathcal{D}(m^2 + 1/4) \pm \Delta\varepsilon(m) - \Delta Hm$ for eigenstate $|1,m\rangle^\pm$, with $\Delta\varepsilon(m) = \sqrt{\mathcal{D}(\mathcal{D}-J)m^2 + (J/4)^2(2S+1)^2}$. Here, $|1,m\rangle^\pm$ is the linear combination of states $|\uparrow\rangle|m-1/2\rangle$ and $|\downarrow\rangle|m+1/2\rangle$.

At low temperature, the transport process is dominated by the sequential tunneling through the SMM energy level, while the co-tunneling and direct tunneling can be neglected safely. For the weak coupling between the SMM and leads, the master equation approach holds. The spin-σ current can be written as $I_\sigma = (I_{{\rm L}\sigma} - I_{{\rm R}\sigma})/2$, where $I_{{\rm L}\sigma}$ ($I_{{\rm R}\sigma}$) represents the spin current flowing from the left (right) lead to the SMM:

$$I_{\alpha\sigma} = -(e/h)\sum_{i,f}(n_i - n_f) R^{f\to i}_{\alpha\sigma} P_f. \tag{3}$$

In Eq. (3), P_i is the probability of finding the SMM in state $|i\rangle$, and $R^{f\to i}_{\alpha\sigma} = \Gamma_{\alpha\sigma}[f(\varepsilon_i - \varepsilon_f - \mu_\alpha)\langle i|c^\dagger_\sigma|f\rangle^2 + f(\varepsilon_i - \varepsilon_f + \mu_\alpha)\langle f|c^\dagger_\sigma|i\rangle^2]$ denotes the transition rate between $|i\rangle$ and $|f\rangle$. $\Gamma_{\alpha\sigma} = 2\pi\rho_{\alpha\sigma}|t_\alpha|^2$ is the line-width function for lead α; $\rho_{\alpha\sigma}$ is the density of states at the Fermi energy, and f_α denotes the Fermi distribution function of lead α with temperature T_α and Fermi energy μ_α. The left electrode is FM metal, with the spin polarization defined as $\mathcal{P}_{\rm FM} = (\rho_{{\rm L}\uparrow} - \rho_{{\rm L}\downarrow})/(\rho_{{\rm L}\uparrow} + \rho_{{\rm L}\downarrow})$. We assume the line-width functions to be $\Gamma_{{\rm L}\uparrow} = \Gamma_0(1 + \mathcal{P}_{\rm FM})$ and $\Gamma_{{\rm L}\downarrow} = \Gamma_0(1 - \mathcal{P}_{\rm FM})$. Here, we take $\mathcal{P}_{\rm FM} \in [0,1]$, representing that the majority electrons are spin-up. The SMM magnetization is defined as $M_{\rm SMM} = \sum_i m_i P_i$. Under low temperature we have $\Delta T \to 0$, then the SMM must be in one of the two bistable ground states $m = \pm S$. For the sake of definition, we set $M_{\rm SMM} = +S$ to be parallel to the magnetization of the left FM lead.

Some techniques that can accurately deal with the time-dependent evolution in SMM systems have been developed,[57,58,66,67] and in this paper, we choose the numerical method suggested in Refs. [41,68,69]. The time evolution can be studied by solving the master equation, which assumes that the kernel does not depend on time.[59] Then, the time dependence of probability $P_i(t)$ can be obtained by solving a series of equations

$$\frac{{\rm d}P_i}{{\rm d}t} = \sum_{f\neq i} P_f R_{f\to i} - P_i \sum_{f\neq i} R_{i\to f}, \tag{4}$$

and steady-state probability $P_i(t\to\infty)$ can be obtained by applying the condition $\mathrm{d}P_i/\mathrm{d}t = 0$. The total tunneling current is $I = \sum_\sigma (I_{\mathrm{L}\sigma} - I_{\mathrm{R}\sigma})/2$, and the spin polarization coefficient of the current is defined as $\eta = (I_\uparrow - I_\downarrow)/I$.

3. Result and discussion

In the following discussions we adopt the parameters based on experiments and first-principles calculations for Mn_{12}-ac molecule[23,31,70] with $S = 10$, $\mathcal{D} = 0.06$ meV, and $U = 25$ meV. This magnetic molecule has two degenerate ground states of $S = \pm 10$ and a relatively large tunneling barrier $\mathcal{D}S^2 \approx 60$ K. The exchange coupling parameter J is taken to be positive ($J = 0.1$ meV), meaning that the coupling is ferromagnetic.[55] Since the next higher energy orbital lies about 8 meV above the LUMO,[71] the higher orbitals are expected to affect the results very weakly in the low-bias voltage regime.

First, we demonstrate how to use a magnetic field to manipulate the HR–LR switching in this SMM-MTJ. Figure 2 shows the magnetization of the SMM and the tunneling current change as functions of the external magnetic field, with a small bias voltage $V = 1.0$ mV exerted across the junction and equilibrium temperature $T = 1$ K. The arrows show the magnetic field scanning direction, and the scanning process is assumed to be slow to ensure that the system can relax to the steady state. As shown in Fig. 2(a), the magnetization of the SMM exhibits a loop structure when the magnetic field is scanned back and forth. The positive applied magnetic field will flip the SMM to the $+S$ (parallel configuration) spin direction, and *vice versa*. Due to the intrinsic magnetism of the SMM, the molecules will preserve their spin states during the gradual reduction of the external magnetic field. Therefore, in the region close to $\Delta H = 0$, both SMM spin states $\pm S$ can be retained. In Fig. 2(b), we plot the electron current as a function of ΔH. If we use I^+ to denote the current when ΔH is scanned from $+3$ meV to -3 meV, and I^- to denote the current when the magnetic field is scanned in the opposite direction, then we can find that the electron tunneling spectra I^+ and I^- are quite different. When the magnetic field ΔH is scanned from $+3$ meV to -3 meV, we observe a large current plateau (LR state) in the window of $\Delta H \in [-0.5, 2]$ meV. This current increases as the spin polarization of the FM electrode increases. When the magnetic field is scanned in the opposite direction, a similar but relatively small current plateau (HR state) appears in the I^- spectrum near $\Delta H \in [-2, 0.5]$ meV, while this current is significantly smaller than I^+ in the LR state. Unlike I^+, a higher spin polarization in the electrode will significantly weaken I^-. Moreover, in the zero-magnetic field (ZF) point ($\Delta H = 0$), the resistance of the molecular junction obviously presents two different states. Both of HR and LR states can be saved at the ZF point. This external magnetic field-controlled HR–LR switching effect is very similar to that in traditional SV devices.[4] The difference is that one of the magnetic layers in the traditional MTJ has been replaced by a magnetic molecule in our system.

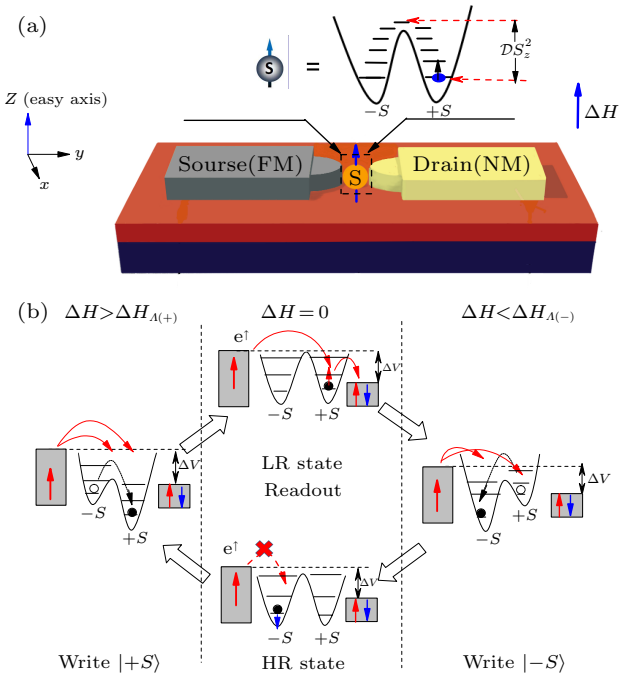


Fig. 1. (a) Schematic diagram of a molecular-MTJ proposed in this paper, which consists of an SMM coupled to an FM lead and an NM lead. (b) Schematic illustration of the "HR–LR" switching by applying an external magnetic field and a small bias voltage.

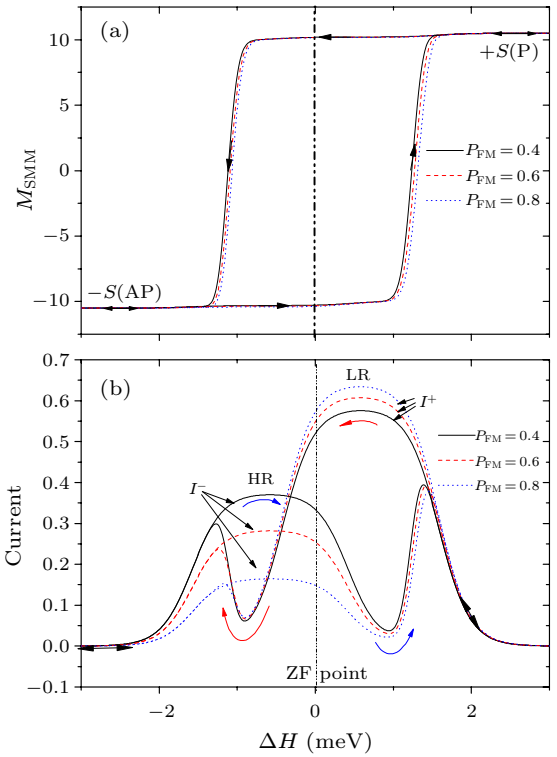


Fig. 2. (a) Magnetic hysteresis loops of the SMM and (b) tunneling currents (scaled by $e\Gamma_0/\hbar$) varying when the external magnetic field ΔH is scanned back and forth, with different lead's spin polarizations. The equilibrium temperature and bias voltage are $T = 1$ K and $V = 1$ mV, respectively.

The HR–LR switching phenomenon illustrated in Fig. 2 can be simply explained as follows: As shown in Fig. 1(b), a magnetic field will destroy the bistable ground states of the SMM, resulting in a change in the SMM magnetic moment. The bias is not large enough to affect the magnetism of the SMM in the absence of a magnetic field. Therefore, in Fig. 2(b), we can observe two different resistance states near the ZF point. If the magnetic field is scanned from +3 meV to 0 meV, then the core spin of the molecule will be flipped by the external magnetic field to the $+S$ spin state (parallel to the magnetism of the FM electrode). Then, the SMM will tend to allow spin-up (majority) electrons in the FM electrode to pass through the junction, and the device will present an LR state. In contrast, if the magnetic field is scanned in the opposite direction, then the antiparallel magnetic configuration will be maintained at the ZF point, and the molecule will favor spin-down (minority) electron flow through the device. As a consequence, an HR state is presented.

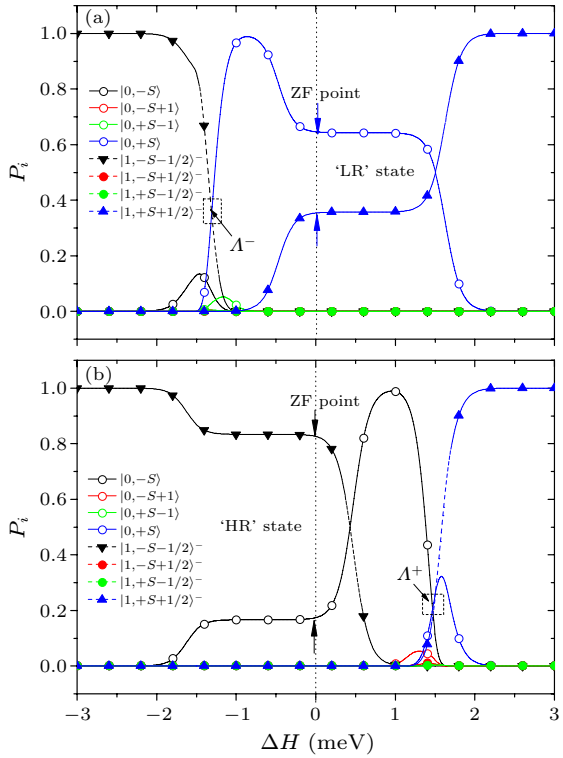


Fig. 3. Variations in the molecular state probabilities (a) as ΔH is scanned from +3 meV to −3 meV and (b) as ΔH is scanned from −3 meV to +3 meV. The equilibrium temperature and bias voltage are given as $T = 1$ K and $V = 1$ mV.

To explain the physical process in Fig. 2 more clearly, we calculate the variation in the probabilities of the SMM states $P_{|0,S-1\rangle}, P_{|0,-S+1\rangle}, P_{|0,\pm S\rangle}, P_{|1,\pm S\pm 1/2\rangle^-}$ and $P_{|1,\pm S\mp 1/2\rangle^-}$ as the magnetic field is scanned back and forth. In Fig. 3(a), the external magnetic field ΔH is slowly scanned from +3 meV to −3 meV to allow the system to relax to the steady state. When $\Delta H > 2.0$ meV, all states are unoccupied except for $|1,+S+1/2\rangle^-$ ($P_{|1,+S+1/2\rangle^-} = 1$), which means that the molecule spin state is pinned in the $+S$ (parallel to the FM electrode) spin direction and that one spin-up electron is trapped in the SMM. Due to the Coulomb repulsion energy of the SMM ($U_{\mathrm{Mn_{12}\text{-}ac}} \approx 25$ meV) and small applied bias voltage, this trapped electron cannot hop into the NM electrode, and the electron current is completely blocked. When ΔH decreases from +2.0 meV to −0.3 meV, the probability $P_{|0,+S\rangle}$ quickly increases, and the tunneling current is dominated by the transition between two states: $|0,+S\rangle \leftrightarrow |1,+S+1/2\rangle^-$. According to Refs. [41,63], only spin-up electrons in this case can tunnel through the LUMO level in the molecule, resulting in a spin-up polarized electron current. Because the FM lead is spin-up polarized, the spin majority (up) electrons are easily transported through the SMM, and an LR state is obtained. If we assume the temperature $T \to 0$, the current in the LR state and ZF condition can be approximated as

$$I_{\mathrm{LR}} \approx \frac{1+\mathcal{P}_{\mathrm{FM}}}{2+\mathcal{P}_{\mathrm{FM}}} e\Gamma_0/\hbar. \tag{5}$$

If ΔH is further decreased to the window of [−2.0 meV, −0.3 meV], then inelastic tunneling processes will occur. In this regime, the bistable energy spectrum of the SMM is completely destroyed, and nearly all the spin states of the molecule have a non-zero probability of being occupied. Among these states, the probabilities of the two special states $|0,+S\rangle$ and $|1,-S-1/2\rangle^-$ are much larger than those of the other states. The point at which $P_{|0,+S\rangle} = P_{|1,-S-1/2\rangle^-}$ exactly corresponds to the magnetism reversal point in Fig. 2(a), indicating that the molecular spin direction starts to reverse from + to − due to the magnetic field. As ΔH continues to vary, all the state probabilities return to 0 except for that of $|1,-S-1/2\rangle^-$ ($P_{|1,-S-1/2\rangle^-} = 1$), which implies that the SMM spin state is pinned in the $-S$ direction and that the tunneling current will be switched "off" by one spin-down electron blocking the electron tunneling channel at the LUMO level. If the magnetic field is scanned in the reverse direction (ΔH changes from −3 meV to +3 meV; see Fig. 3(b)), then similar physical phenomena will occur. The SMM magnetic reversal point from − to + corresponds to the point where $P_{|0,-S\rangle} = P_{|1,+S+1/2\rangle^-}$, and the electron tunnelling process in the HR window is dominated by the transition $|1,-S-1/2\rangle^- \leftrightarrow |0,-S\rangle$, which means that only spin minority (down) electrons can flow through the molecule. At low temperatures, the spin-down polarized electron current in the HR state and ZF condition yields

$$I_{\mathrm{HR}} \approx \frac{1-\mathcal{P}_{\mathrm{FM}}}{2-\mathcal{P}_{\mathrm{FM}}} e\Gamma_0/\hbar. \tag{6}$$

If we define a parameter $\mathrm{MR} = \frac{I_{\mathrm{LR}}-I_{\mathrm{HR}}}{I_{\mathrm{HR}}}$ to describe the on-off ratio of LR-HR switching, then the MR ratio under low temperature and ZF condition can be given as

$$\mathrm{MR} = \frac{2\mathcal{P}_{\mathrm{FM}}}{2-\mathcal{P}_{\mathrm{FM}}-\mathcal{P}_{\mathrm{FM}}^2}. \tag{7}$$

Similar to the results of the Jullière's model,[1] from Eq. (7) we can determine that the MR ratio mainly depends on the spin polarization of the electrode. The higher the spin polarization of the FM lead is, the greater the MR ratio of the device, and the better the device functions as an SV device.

Next, we discuss the effect of the equilibrium temperature on this device. For ease of description, we use Λ^- to denote the reversal point when the spin state of the SMM switches from $+$ to $-$ and Λ^+ to denote the reversal point from $-$ to $+$. As shown in Fig. 4(a), the magnetic hysteresis loop shrinks and the distance between Λ^+ and Λ^- decreases with increasing temperature. As mentioned in regard to Fig. 3, the magnetism reversal point Λ^+ corresponds to the point where $P_{|0,-S\rangle} = P_{|1,+S+1/2\rangle}$, and Λ^- corresponds to another point where $P_{|0,+S\rangle} = P_{|1,-S-1/2\rangle^-}$. Therefore, in Fig. 4(c), we plot the state probabilities $P_{|0,S\rangle}$ and $P_{|1,-S-1/2\rangle^-}$ as functions of ΔH when the magnetic field is scanned from $+3$ meV to -3 meV under different equilibrium temperatures. As shown in Fig. 4(c), a higher temperature will excite these two states to participate in the transition earlier, which will lead to the molecular magnetic moment being more prone to flipping. As a result, the absolute values of Λ^+ and Λ^- will decrease with increasing temperature. In addition, with decreasing temperature, the shape of the current spectra in the HR and LR states gradually evolves into a plateau. We take the current in the LR state as an example. As discussed in regard to Fig. 3, the current in the LR state is dominated by the transition $|0,+S\rangle \leftrightarrow |1,+S+1/2\rangle^-$. Therefore, in Fig. 4(d), we plot the probabilities of these states as functions of ΔH. A lower temperature causes the electron tunneling process to be more easily dominated by the transition between the two states $|0,+S\rangle$ and $|1,+S+1/2\rangle^-$, resulting in the gradual evolution of the current distribution into a plateau. In contrast, a higher temperature will excite more spin states to participate in the tunneling process, which will reduce the spin polarization of the current and, to a certain extent, narrow the LR (HR) state window.

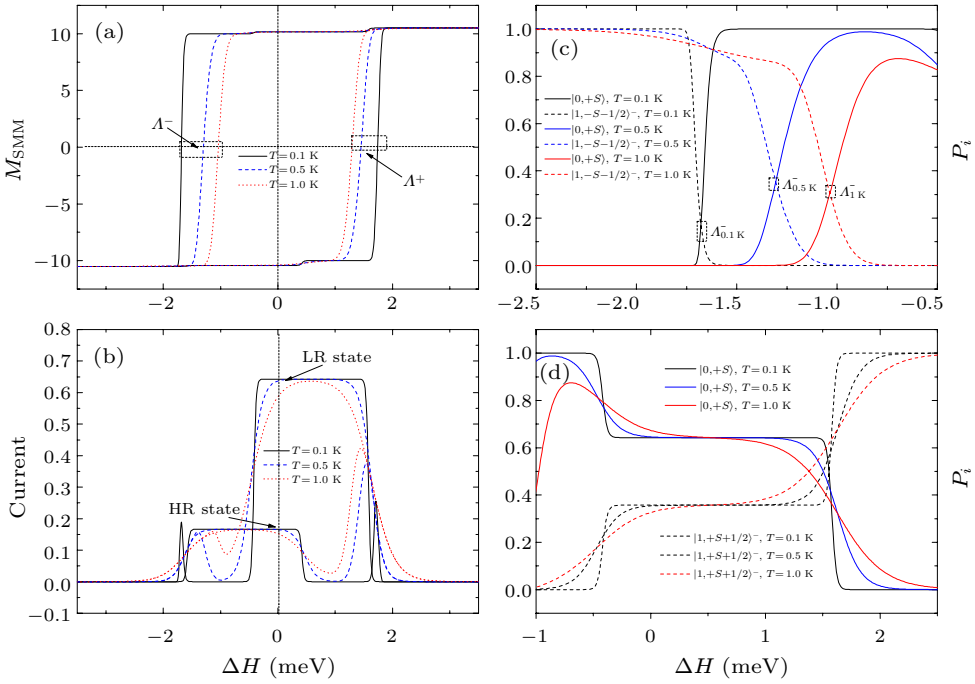


Fig. 4. (a) Magnetic hysteresis loops of the SMM and (b) tunneling currents (scaled by $eI_0/\hbar$) varying when the external magnetic field ΔH is scanned back and forth, with different temperature and bias $V = 1.0$ mV. (c) and (d) Variations in the molecular state probabilities (c) $P_{|0,+S\rangle}$ and $P_{|1,-S-1/2\rangle^-}$ and (d) $P_{|0,+S\rangle}$ and $P_{|1,+S+1/2\rangle}$ as ΔH is scanned from $+3$ meV to -3 meV.

Finally, let us discuss how to implement the device scheme proposed in this paper under a real experimental environment. In Fig. 5, we use a time-varying magnetic field with an amplitude $\Delta H = \pm 0.8$ meV (approximately 5.5 T) to "write" the resistance state in this device. According to the experimental work of Jo *et al.*,[72] such a magnetic field can be achieved under the current experimental conditions. The train of magnetic field signals applied to the SMM periodically changes its direction every $2 \times 10^5\ \hbar/\Gamma$ ($\cong 4$ μs for $\Gamma = 8$ GHz[69]). As shown in Fig. 5(a), this time-varying magnetic field signal only lasts 2 μs every time to reach ± 0.8 meV and then quickly reduces to zero. Figure 5(c) shows that the SMM can maintain its magnetization (remain in the $+S$ or $-S$ spin state) when the magnetic field disappears. To detect the HR–LR switching in this device, we apply a small bias voltage $V = 0.5$ mV across the two electrodes. As shown in Fig. 5(b), we calculate the current spectrum changes with the magnetic field variation. The tunneling current can clearly be switched between the "HR" and "LR" state by this time-varying external magnetic field. Even with a relatively low spin-polarized

FM electrode ($P_{\rm FM} = 0.3$, close to the spin polarization of the metal Ni[73,74]) and higher temperature $T = 2$ K, the MR ratio at ZF point can reach almost 0.38, which is very consistent with the prediction of Eq. (7). Interestingly, every time the sign of the magnetic signal changes, the electron current obviously oscillates and soon stabilizes to a new plateau. This unusual electrical signal is instantaneous and disappears with the completion of the molecular magnetic inversion process. Therefore, observing the generation and disappearance of this signal may yield effective evidence to judge whether magnetic reversal of the molecular magnetism has been completed. Furthermore, as shown in Fig. 5(d), regardless of how the polarization of the FM electrode changes, the spin polarization parameter of the electron current η can always vary from $+1$ to -1. This shows that not only the resistance state but also the current spin polarization parameter in this system can be rewritten by a magnetic field.

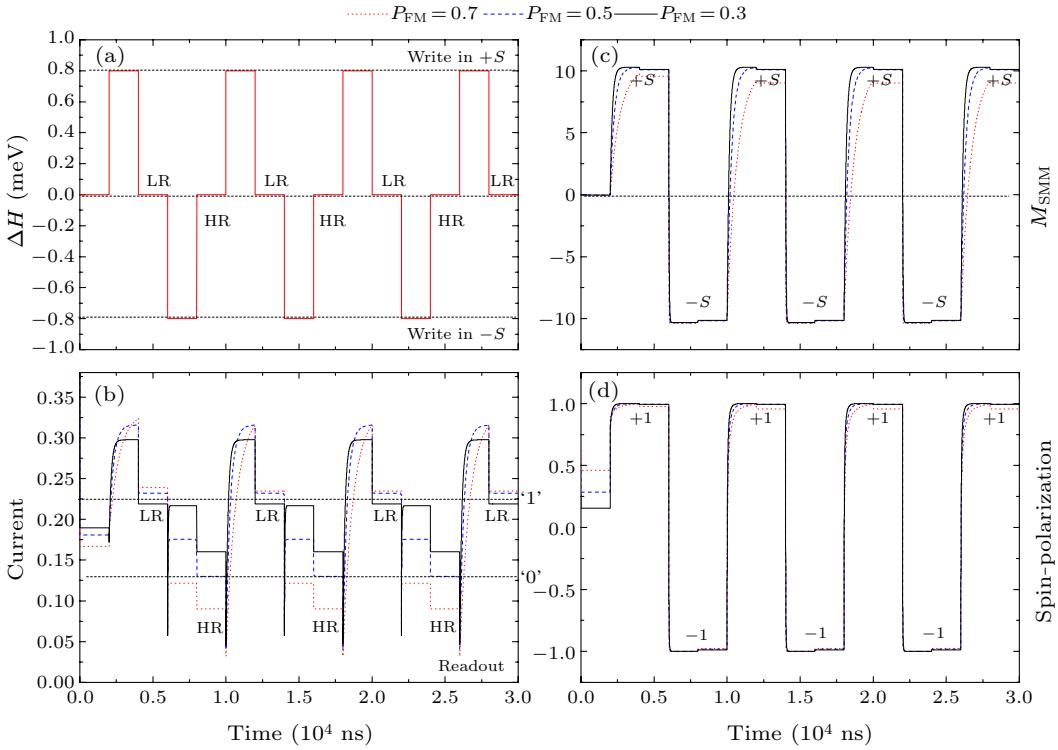


Fig. 5. (b) Electron current, (c) molecule's magnetism $M_{\rm SMM}$ and (d) current's spin polarization coefficient η response of an alternate series of magnetic field (a) of $+0.8$ meV and -0.8 meV, with different spin polarizations of FM lead. The initial states are prepared as $P_{|\pm S\rangle} = 0.5$ and $\varepsilon_0 = 1$ meV. The equilibrium temperature and bias voltage are set to $T = 2$ K and $V = 0.5$ mV.

4. Conclusions

In summary, we have proposed a supramolecular SV consisting of an SMM and an FM electrode. By adjusting the magnetic field, the core spin of the molecule can be switched between two bistable magnetic ground states $|\pm S\rangle$, leading to a parallel (LR) or an antiparallel (HR) magnetic configuration of the system. Our numerical results show that the device resistance depends on the spin alignment of the MTJ, which can be controlled by an external magnetic field and read out by a small bias voltage. More interestingly, due to the intrinsic magnetism of the SMM, this HR/LR state can be saved and readout under a ZF condition. The results in this work offer a starting point to study multilayer structures combined with molecular magnets, such as SMM spin-valve structures. However, the functional ability of the device greatly depends on the molecular magnetic characteristics, a relatively low equilibrium temperature and an FM electrode.

Acknowledgments

This work was supported by the National Natural Science Foundation of China (Grant No. 11404322), the Natural Science Foundation of Huai'an (Grant Nos. HAB202229 and HAB202150), and the Natural Science Foundation of the Jiangsu Higher Education Institutions of China (Grant No. 22KJD140002).

References

[1] Žutiá I, Fabian J and Sarma S D 2004 *Rev. Mod. Phys.* **76** 323
[2] Yasuhiro F, Le W, Hiroshi I, Saburo T, Sadamichi M and Chika O Y 2011 *Nat. Mater.* **10** 527
[3] Park B G, Wunderlich J, Marti X, Holy V, Kurosaki Y, Yamada M, Yamamoto H, Nishide A , Hayakawa J, Takahashi H, Shick A B and Jungwirth T 2011 *Nat. Mater.* **10** 347
[4] Jedema F J, Filip A T and van Wees B J 2001 *Nature* **410** 345
[5] Dieny B 1991 *Phys. Rev. B* **43** 1297
[6] Baibich M N, Broto J M, Fert A, Nguyen Van Dau F, Petroff F, Etienne P, Creuzet G, Friederich A and Chazelas J 1988 *Phys. Rev. Lett.* **61** 2472

[7] Moodera J, Kinder L, Wong T and Meservey R 1995 *Phys. Rev. Lett.* **74** 3273
[8] Prigodin V N, Raju N P, Pokhodnya K I, Miller J S and Epstein A J 2002 *Adv. Mater.* **14** 1230
[9] Nguyen T D, Ehrenfreund E and Vardeny Z V 2012 *Science* **337** 204
[10] Xiong Z H, Wu D, Vardeny Z V and Shi J 2004 *Nature* **427** 821
[11] Yoo J W, Chen C Y, Jang H W, Bark C W, Prigodin V N, Eom C B and Epstein A J 2010 *Nat. Mater.* **9** 638
[12] Ma Y J, Hu J X, Han S D, Pan J, Li J H and Wang G M 2020 *J. Am. Chem. Soc.* **142** 2682
[13] Li Y Q, Kan H J, Miao Y Y, Yang L, Qiu S, Zhang G P, Ren J F, Wang C K and Hu G C 2020 *Chin. Phys. B* **29** 017303
[14] Thomas L, Lionti F, Ballou R, Gatteschi D, Sessoli R and Barbara B 1996 *Nature* **383** 145
[15] Escalera-Moreno L, Baldov J J, Gaita-Ario A and Coronado E 2018 *Chem. Sci.* **9** 3265
[16] Gaita-Ario A, Luis F, Hill S and Coronado E 2019 *Nat. Chem.* **11** 301
[17] Guo F S, Day B M, Chen Y C, Tong M L, Mansikkamki A and Layfield R A 2018 *Science* **362** 6421
[18] Leuenbergerand M N and Loss D 2001 *Nature* **410** 789
[19] Zyazin A S, van den Berg J W G, Osorio E A, van der Zant H S J, Konstantinidis N P, Leijnse M, Wegewijs M R, May F, Hofstetter W, Danieli C and Cornia A 2010 *Nano Lett.* **10** 3307
[20] Gaudenzi R, Misiorny M, Burzur E, Wegewijs M R and van der Zant H S J 2017 *J. Chem. Phys.* **146** 092330
[21] Chen Y C and Tong M L 2022 *Chem. Sci.* **13** 8716
[22] Shao D and Wang X Y 2020 *Chin. J. Chem.* **38** 1005
[23] Andoni Z, Jose M S and Enrique C 2021 *Coordinat. Chem. Rev.* **441** 213984
[24] Wang J H, Lia Z Y, Yamashita M and Bu X H 2021 *Coordinat. Chem. Rev.* **428** 213617
[25] Prins F, Monrabal-Capilla M, Osorio E A, Coronado E and van der Zant H S J 2011 *Adv. Mater.* **23** 1545
[26] Meded V, Bagrets A, Fink K, Chandrasekar R, Ruben M, Evers F, Bernand-Mantel A, Seldenthuis J S, Beukman A and van der Zant H S J 2011 *Phys. Rev. B* **83** 245415
[27] Alam M S, Stocher M, Gieb K, Muller P, Haryono M, Student K and Grohmann A 2010 *Angew. Chem. Int. Ed.* **49** 1159
[28] Voss S, Fonin M, Rudinger U, Burgert M and Groth U 2007 *Appl. Phys. Lett.* **90** 133104
[29] Gehring P, Thijssen J M and van der Zant H S J 2019 *Nat. Rev. Phys.* **1** 381
[30] Czap G, Wagner P J, Xue F, Gu L, Li J, Yao J, Wu R Q and Ho W 2019 *Science* **364** 670
[31] Heersche H B, de Groot Z, Folk J A, van der Zant H S J, Romeike C, Wegewijs M R, Zobbi L, Barreca D, Tondello E and Cornia A 2006 *Phys. Rev. Lett.* **96** 206801
[32] Barraza-Lopez S, Park K, Garca-Suárez V and Ferrer J 2009 *Phys. Rev. Lett.* **102** 246801
[33] Barraza-Lopez S, Park K, Garca-Suárez V and Ferrer J 2009 *J. Appl. Phys.* **105** 07309
[34] Gu L and Wu R Q 2020 *Phys. Rev. Lett.* **125** 117203
[35] Gu L and Wu R Q 2021 *Phys. Rev. B* **103** 014401
[36] Pei T, Thomas J O, Sopp S, Tsang M Y, Dotti N, Baugh J, Chilton N F, Cardona-Serra S, Gaita-Ario A , Anderson H L and Bogani L 2022 *Nat. Commun.* **13** 4506
[37] Hymas K and Soncini A 2019 *Phys. Rev. B* **99** 245404
[38] Pominska A and Weymann I 2015 *Phys. Rev. B* **92** 205419
[39] Nossa J F, Islam M F, Canali C M and Pederson M R 2013 *Phys. Rev. B* **88** 224423
[40] Fransson J, Ren J and Zhu J X 2014 *Phys. Rev. Lett.* **113** 257201
[41] Timm C and Elste F 2006 *Phys. Rev. B* **73** 235304
[42] Pominska A and Weymann I 2016 *Phys. Rev. B* **94** 035422
[43] Misiorny M, Weymann I and arnaś J 2010 *Europhys. Lett.* **89** 18003
[44] Hu G C, Zhang Z, Zhang G P, Ren J F and Wang C K 2016 *Org. Electron.* **37** 485
[45] Hammar H, Jaramillo J D V and Fransson J 2019 *Phys. Rev. B* **78** 115416
[46] Wang R Q, Sheng L, Shen R, Wang B G and Xing D Y 2010 *Phys. Rev. Lett.* **105** 057202
[47] Zhang Z Z, Jiang L, Wang R Q, Wang B G and Xing D Y 2011 *Appl. Phys. Lett.* **99** 133110
[48] Misiorny M and Barnaś J 2007 *Phys. Rev. B* **76** 054448
[49] Zhang Z Z and Jiang L 2014 *Nanotechnology* **25** 365201
[50] Alez G G, Leuenberger M N and Mucciolo E R 2008 *Phys. Rev. B* **78** 054445
[51] Romeike C, Wegewijs M R, Hofstetter W and Schoeller H 2006 *Phys. Rev. Lett.* **96** 196601
[52] Li Y Q, Kan H J, Miao Y Y, Qiu S, Zhang G P, Ren J F, Wang C K and Hu G C 2020 *Physica E* **124** 114327
[53] Serrano G, Poggini L, Briganti M, Sorrentino A L, Cucinotta G, Malavolti L, Cortigiani B, Otero E, Sainctavit P, Loth S, Parenti F,Barra A-L, Vindigni A, Cornia A, Totti F, Mannini M and Sessoli R 2020 *Nat. Mater.* **19** 546
[54] Bogani L and Wernsdorfer W 2008 *Nat. Mater.* **7** 179
[55] Urdampilleta M, Klyatskaya S, Cleuziou J P, Ruben M and Wernsdorfer W 2011 *Nat. Mater.* **10** 502
[56] Sanvito S 2011 *Nat. Mater.* **10** 484
[57] Pominska A, Misiorny M and Weymann I 2017 *Phys. Rev. B* **95** 155446
[58] Pominska A, Misiorny M and Weymann I 2018 *Phys. Rev. B* **97** 035415
[59] Pominska A, Misiorny M and Weymann I 2018 *Europhys. Lett.* **121** 38006
[60] Xie H, Wang Q, Xue H B, Jiao H J and Liang J Q 2013 *J. Appl. Phys.* **113** 213708
[61] Misiorny M, Weymann I and Barnaś J 2009 *Phys. Rev. B* **79** 224420
[62] Misiorny M and Barnaś J 2007 *Phys. Rev. B* **75** 134425
[63] Elste F and Timm C 2006 *Phys. Rev. B* **73** 235305
[64] Elste F and Timm C 2007 *Phys. Rev. B* **75** 195341
[65] Misiorny M and Barnaś J 2007 *Phys. Rev. B* **77** 172414
[66] Hammar H and Fransson J 2016 *Phys. Rev. B* **94** 054311
[67] Wrzesniewski K and Weymann I 2020 *Phys. Rev. B* **101** 245434
[68] Timm C and Ventra M D 2012 *Phys. Rev. B* **86** 104427
[69] Lu H Z, Zhou B and Shen S Q 2009 *Phys. Rev. B* **79** 174419
[70] Rogez G, Donnio B, Terazzi E, Gallani J L, Kappler J P, Bucher J P and Drillon M 2009 *Adv. Mater.* **21** 4323
[71] Timm C 2007 *Phys. Rev. B* **76** 014421
[72] Jo M H, Grose J E, Baheti K, Deshmukh M M, Sokol J J, Rumberger E M, Hendrickson D N, Long J R, Park H and Ralph D C 2006 *Nano Lett.* **6** 2014
[73] Yoshida K, Hamada I, Sakata S, Umeno A, Tsukada M and Hirakawa K 2013 *Nano Lett* **13** 481
[74] Hamaya K, Kitabatake M, Shibata K, Jung M, Kawamura M, Ishida S, Taniyama T, Hirakawa K, Arakawa Y and Machida T 2008 *Phys. Rev. B* **77** 081302